

Ferrospheres from Fly Ashes: Composition and Catalytic Properties in High-Temperature Oxidation of Methane

Alexander G. Anshits^{1,2}, Olga M. Sharonova¹, Natalia N. Anshits^{1,2},
Sergei N. Vereshchagin¹, Evgenii V. Rabchevskii¹, and Leonid A.
Solovjev¹

¹Institute of Chemistry and Chemical Technology, Siberian Branch, Russian Academy of Sciences, ul. Karla Marksa 42, Krasnoyarsk, 660049 Russia; ²Siberian Federal University, Svobodny pr. 79, Krasnoyarsk, 660041 Russia

KEY WORDS: ferrospheres, catalysis, oxidation, methane

ABSTRACT

A systematic investigation the relationship between the composition, morphology, structural characteristics of iron-containing phases, and catalytic properties of narrow fractions of ferrospheres separated from four known types of fly ashes has been performed. It has been established that the major component compositions of all the studied narrow fractions of ferrospheres and magnetic concentrates obtained from 14 heat and electric power plants in Russia, Ukraine, and Kazakhstan are described by two general linear regression equations $[\text{SiO}_2] = 65.71 - 0.71 \cdot [\text{Fe}_2\text{O}_3]$ and $[\text{Al}_2\text{O}_3] = 24.92 - 0.26 \cdot [\text{Fe}_2\text{O}_3]$ with correlation coefficients of -0.99 and -0.97 , respectively.

In the general dependence of the Fs composition, there are two regions different in the properties of the melt from which the ferrospheres are formed. In a wide range of variations in the iron concentration $C_{\text{Fe}} = 25\text{--}55$ wt %, the behavior of the melt is determined by the properties of the $\text{FeO}\text{--}\text{SiO}_2\text{--}\text{Al}_2\text{O}_3\text{--}\text{CaO}$ system. For higher iron concentrations $C_{\text{Fe}} > 55$ wt % and low contents of Al_2O_3 and SiO_2 (< 1 wt %), the behavior of the melt is determined by the properties of the $\text{FeO}\text{--}\text{CaO}$ system.

The first composition region is characterized by the formation of aluminum magnesium ferrite spinel. The content of the ferrosphenel increases with increasing iron concentration, and the unit cell parameter of the ferrosphenel changes in the range $8.344\text{--}8.3897$ Å. The activity of the Fs in the reaction of deep oxidation of methane is determined by the ferrosphenel concentration and the content of the amorphous phase in narrow fractions of Fs. The high content of the amorphous phase leads to a blocking of the catalytically active ferrosphenel and to a decrease in the activity of the ferrospheres. The $\text{FeO}\text{--}\text{CaO}$ system is characterized by the formation of CaO -promoted ferrite spinel, which has the unit cell parameter exceeding the corresponding parameter of stoichiometric magnetite, and by the formation of defect $\alpha\text{-Fe}_2\text{O}_3$ with the surface enriched in CaO . The drastic change observed in the catalytic properties of ferrospheres in this system is explained

by the enrichment of the surface of iron-containing CaO phases and by the formation of defect centers responsible for the high selectivity in the reaction of oxidative dimerization of methane.

1. INTRODUCTION

Among the most commonly encountered modifications of microspherical components of fly ashes obtained from the pulverized combustion of different types of coals from heat and electric power plants are ferrospheres (Fs) characterized by a high iron content. The formation of their globular structure occurs as a result of the thermochemical conversion of original mineral forms of coals with the formation of droplets of high-iron melts of the complex (FeO–CaO–MgO–SiO₂–Al₂O₃) major component composition, the partial crystallization, and the oxidation of individual phases during their cooling. The granulometric, chemical, and phase compositions of the ferrosphere concentrates, as well as the size of crystallites of incipient mineral phases and the morphology of globules, depend on a large number of parameters, including the composition of the original coal, the regime of its combustion, the conditions used for cooling melt droplets, etc.¹⁻⁴.

The formation of ferrospheres occurs with the participation of not only the sulfide and carbonate forms of iron but also the organomineral forms involved in the composition of coals. The mobilization of mineral iron forms of the original coals is proved by a clear correlation ($r = 0.965$) between the content of ferrospheres in fly ashes and the content of iron in coals from 23 heat and electric power plants in Russia, Ukraine, and Kazakhstan, which have burnt brown coals, bituminous coals, and anthracites with different mineral forms of iron. The free term in the regression equation ($Fs = 2.92 \cdot Fe_{\text{coal}} - 2.33$), probably, characterizes the part of the iron which does not participate in the formation of ferrospheres, for example, the iron involved in the composition of hydromica³.

The analysis of the data available in the literature has demonstrated that the vast majority of studies performed so far in this field have been devoted to the investigation of the concentrates or total magnetic fractions isolated by magnetic separation of dry fly ashes, narrow fractions of ashes, or feed pulp with the use of a hand magnet^{3, 5-11}. In this case, the yield of magnetic fractions from fly ashes obtained from the combustion of different types of coals is equal to 0.5–18.1%, the iron content in these fractions varies in the range 20–88 wt % Fe₂O₃, and the size of globules lies in the range from two or three to several hundred micrometers with a maximum of the particle size distribution in the range from 40 to 150 μm (for different sources).

Magnetic fractions from different sources are multiphase systems including magnetite, hematite, and Ca–Mg ferrite spinels as the main phases and smaller amounts of maghemite, martite, muscovite, wustite, ilmenite, chromite, natural Fe,Mn-ferrite, ferrosilicium, iron hydroxides, and iron silicates. Moreover, the magnetic fractions contain the glass phase, quartz, anhydrite gypsum, potassium feldspar, porcelain clay, mica, mullite, carbonates, periclase, and Cr–Ni spinel, which are associated with the

main iron-containing phases¹⁻¹². Multiple magnetic cleaning and washing with water have been used to remove low-density impurities (aluminosilicate, char particles, gypsum) and to increase the total content of iron in concentrates of ferrospheres. This also leads to a narrowing of the phase composition, which, as the main phases, includes magnetite, hematite, maghemite, quartz, mullite, and the glass phase³.

Since concentrates of Fs from different sources have a variable composition and, as a consequence, exhibit unstable and unpredictable properties, they can be widely used only as raw materials in metallurgy instead of natural magnetites, weighting materials for mineral suspensions in concentration of ores and preparation of coals¹³⁻¹⁶, fillers of special concretes in building of nuclear power plants¹⁷, and as lake pigment components¹⁸.

At the same time, the microspherical design and unique combination of magnetic properties, high thermal stability, and mechanical strength make Fs concentrates attractive for the use as modern functional materials, which can replace expensive synthetic ones. In particular, narrow fractions of ferrospheres have found application as microspherical magnetic carriers with a surface reactivity up to 500 $\mu\text{mol OH/g}$, which have been used in the synthesis of sorbents with chemically bound bioluminescence and fluorescence proteins and cells¹⁹. Moreover, it has been demonstrated that narrow fractions of ferrospheres can be used for decomposing liquid radioactive wastes based on tributyl phosphate with the formation butenes and immobilization of radionuclides in the composition of iron phosphate ceramics²⁰.

However, the most promising application of ferrospheres seems to be their use as catalysts in the processes where expensive traditional systems either are unstable or are rapidly deactivated under the action of harmful impurities contained in raw materials or high temperatures providing the occurrence of the reactions involved. In particular, ferrospheres exhibit a high efficiency in thermolysis of heavy oils and petroleum residues into components of motor fuels^{21, 22}, as well as in the processes of high-temperature oxidation and oxidative dimerization of methane²³⁻²⁵.

The use of ferrospheres as catalysts in the high-temperature process of oxidative dimerization of methane with the formation of ethylene, although offers obvious advantages, also involves serious problems associated with variations in the complex multicomponent composition of the $\text{Fe}_2\text{O}_3\text{-Al}_2\text{O}_3\text{-SiO}_2\text{-CaO}$ system. It is clear that, for such systems, unambiguous conclusions regarding the nature of the catalytically active phase can be drawn only based on the results of a systematic investigation of a number of samples with revealing and elucidating the composition–structure–property relationship.

The purpose of this work is to reveal and elucidate the general regularities of the relationship between the major component and phase compositions, morphology, structural characteristics of iron-containing phases, and catalytic properties of narrow fractions of ferrospheres in high-temperature oxidation of methane.

2. EXPERIMENTAL

2.1. Original Ashes

Ferrospheres were separated using fly ashes obtained from the pulverized combustion of coals of different grades from five deposits, including three large coal basins, namely, Kansk-Achinsk, Kuznetsk, and Ekibastuz Basins (Russia). The coals are different in the technological types and, consequently, in the reactivity^{26–29}, which determines different types of boiler units and different temperature regimes of their operation. Coals of the low grade, i.e., brown coals of the B2 grade (subC) and hard coals of the grades D and DG (hvBb), exhibit a high reactivity; therefore, they have been burnt in dry-ash-removal units at lower temperatures (1100–1400°C). In contrast to the low-grade coals, the high-grade coals, i.e., hard coals of the grades SS (mvb) and T (sa), exhibit a low reactivity. They have been burnt in slag-tap units at higher temperatures (1500–1700°C).

According to the paper³⁰, the fly ashes obtained from the combustion of coals of different grades are significantly different in the mineral composition and belong to different “chemical” types. Ferrospheres of the series E and P2 were prepared from fly ashes of the S type; ferrospheres of the series B1, from fly ashes of the FS type; and ferrospheres of the series K2 and S1, from fly ashes of the CS and FCS types. In this case, the fly ashes used to prepared ferrospheres of the S1 series are characterized by a higher calcium content as compared to the ferrospheres of the K2 series.

2.2. Preparation of Narrow Fractions of Ferrospheres

Ferrospheres were prepared using the procedure described in³¹, according to which the magnetic concentrate obtained from the fly ash was subjected to grain-size classification with the separation of narrow fractions of specified sizes. In turn, each fraction was subjected to separate enrichment and purification from nonmagnetic impurities with the use of the dry and wet magnetic separation techniques in fields of different strengths, hydrodynamic gravitational separation, and final sizing. The separation of ferrospheres into fractions makes it possible (i) to decrease the contamination of small fractions of microspheres by fragments of large fractions, (ii) to choose more effective regimes for magnetic separation and hydrodynamic gravitational separation of narrow fractions, and (iii) to purposefully obtain the final products with specified sizes, compositions, and properties. The schematic diagram illustrating the processing of fly ashes for the preparation of ferrospheres is shown in Fig. 1.

Small fractions (with sizes < 0.1 mm) were subjected to hydrodynamic gravitational separation (HS) in a pulsed ascending turbulent water stream³², which made it possible to destroy agglomerates of finely dispersed particles and to effectively separate them in density. In order to increase the purity of the magnetic products of large fractions of the series E, P2, and K2, as well as the heavy products of the hydrodynamic gravitational separation of all fractions of the B series, we used an additional wet magnetic separation (WMS) on an experimental electromagnetic tubular separator in a magnetic

field with an induction less than 0.3 T. The final stage for all fractions (except the fraction with sizes < 0.05 mm) was the final sizing.

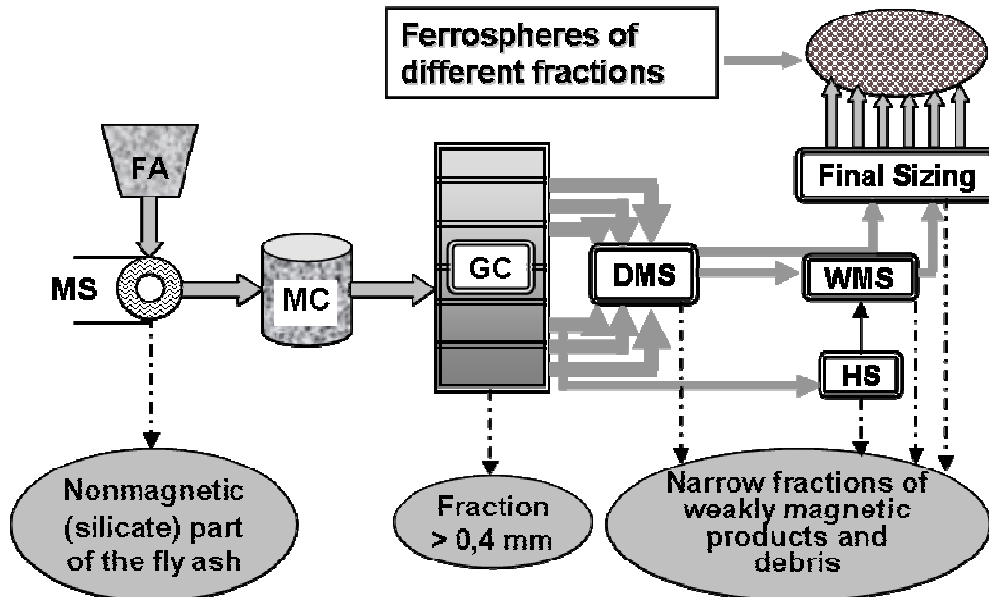


Fig. 1. Block diagram showing generation of different narrow fractions of ferrospheres: FA is fly ash, MS is magnetic separation, MC is magnetic concentrate, GC is grain-size classification, DMS is dry magnetic separation, WMS is wet magnetic separation, and HS is hydrodynamic separation.

2.3. Experimental Methods

The purity of the fractions obtained was controlled using an Axioscop-40 optical microscope (Carl Zeiss, Germany) equipped with a digital color video camera (Canon) (Fig. 2).

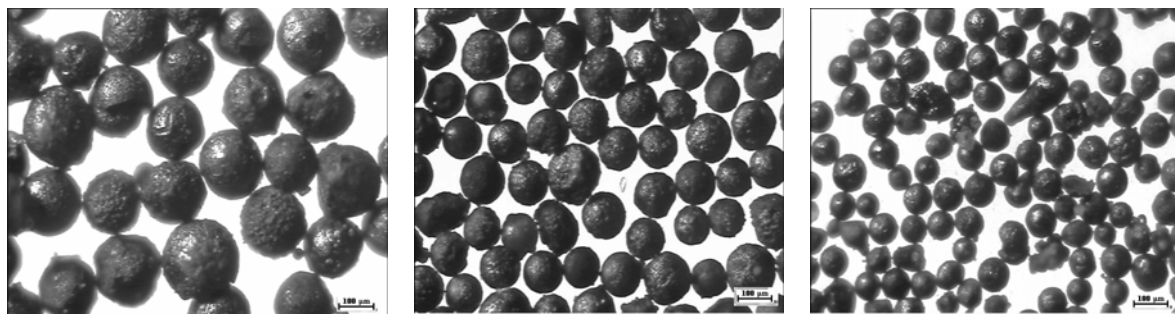


Fig. 2. Optical microscopy micrographs of ferrospheres narrow fractions (a) $-0,2+0,16$ mm; (b) $-0,16+0,1$ mm and (c) $-0,063+0,05$ mm

High-fluidity microspherical materials were investigated using conventional techniques of sampling³³ and chemical analysis³⁴ with the standard error in the resettability of results for the major components depending on their content, i.e., $S_n = \pm 0.35$ to ± 0.60

for SiO₂; ±0.30 to ±0.40 for Al₂O₃; ±0.15 to ±0.30 for Fe₂O₃; and ±0.04 to ±0.10 for Ca, Mg, Na, K, and Ti oxides. The bulk density was determined according to the standard procedure described in the paper ³⁵. The samples were manually compacted to the normalized volume. The bulk density was calculated as the arithmetic mean of the results of three to five measurements. The granulometric composition of the magnetic concentrates was determined by dry screening of the sample according to the standard ³⁶ using a VP-S/220 vibrodrive with a set of sieves with meshes 0.4; 0.2; 0.16; 0.1; 0.063; and 005 mm.

The quantitative phase composition of the ferrospheres was determined using the X-ray powder diffraction analysis with the full-profile Rietveld method ³⁷ and the derivative difference minimization ³⁸. The X-ray powder diffraction patterns were recorded in the reflection geometry on a PANalytical X'Pert PRO diffractometer (Co K α radiation, graphite monochromator, scan range 2 θ =15–115°) equipped with a PIXcel detector. The content of the X-ray amorphous component in weight percent was determined by the external standard method with hematite used as the external standard. The absorption coefficients of the samples for Co K α radiation were calculated from the total elemental composition according to the chemical analysis data. The reproducibility of the results was controlled using the external standard (NaCl), which was mixed in some samples.

The specific surface area of the samples was determined by thermal desorption of argon according to the multipoint Brunauer–Emmett–Teller (BET) method (NOVA 3200e instrument) or by thermal desorption of nitrogen according to the single-point BET method (Gazokhrom-1 instrument).

The catalytic properties of narrow fractions of ferrospheres were studied in a HECTOR continuous-flow multi-cell reactor catalytic setup with the chromatographic determination of the compositions of the initial mixture and the products of methane conversion. The experiments were performed at temperatures of 600–750°C with a reaction mixture of the composition CH₄ : O₂ : N₂ = 82 : 9 : 9 vol % at a total pressure of 1.3 atm. The weighed portion of the catalyst was equal to 0.30–0.33 g, and the volume feed rate of the mixture was 15 cm³/min (NTP). The temperature dependence of the activity was investigated during heating of the catalysts in a flow of the reaction mixture sequentially to temperatures of 600, 650, 700, and 750°C with exposure to each temperature for about 4 h (15 h at 700°C).

3. RESULTS AND DISCUSSION

The use of the three-stage separation scheme, including the dry and wet magnetic separation, grain-size classification, and hydrodynamic separation of small fractions from foreign impurities made it possible to obtain 24 homogeneous narrow fractions of ferrospheres with different sizes from the fly ashes, which, according to their composition, belong to different classes S, CS, FS, and FCS. The chemical compositions of the narrow fractions of Fs are presented in Table 1. For the products obtained, we determined the true and bulk densities and the specific surface area. The

Table 1. Chemical composition and bulk density of narrow ferrospheres fractions

Series, fraction	Bulk density, g/cm ³	Chemical composition, wt %									
		L.O.I.	SiO ₂	Al ₂ O ₃	Fe ₂ O ₃	CaO	MgO	Na ₂ O	K ₂ O	TiO ₂	SO ₃
Series P2											
P2 -0.4+0.2	-	0.00	34.16	12.15	43.82	5.33	2.01	0.69	0.86	0.30	0.32
P2 -0.2+0.16	0.89	0.00	41.60	15.21	30.04	6.13	2.95	0.80	1.18	0.49	0.40
P2 -0.16+0.1	0.86	2.11	37.67	12.96	37.47	5.81	2.92	0.66	0.66	0.23	0.22
P2 -0.1+0.063	1.29	1.58	33.90	8.82	48.93	2.94	3.38	0.75	0.45	0.00	0.05
P2 -0.063+0.05	1.59	0.00	23.84	8.52	61.42	3.17	2.87	0.80	0.40	0.00	0.05
P2 -0.05	1.69	0.12	20.70	6.62	66.38	2.94	2.82	0.80	0.40	0.05	0.04
Series E											
E -0.4+0.2	0.81	2.56	39.70	15.92	36.26	3.69	1.38	0.40	0.26	1.14	0.60
E -0.2+0.16	0.85	1.70	36.91	15.16	41.26	3.25	1.64	0.80	0.26	1.15	0.71
E -0.16+0.1	0.96	1.26	38.40	16.32	39.31	2.82	1.61	0.25	0.20	1.03	0.46
E -0.1+0.063	1.13	0.32	33.08	12.74	49.28	2.71	1.15	1.18	0.26	1.28	0.62
E -0.063+0.05	1.35	0.00	26.48	9.44	59.82	2.82	1.08	0.94	0.20	1.40	0.67
E -0.05	1.66	0.00	19.20	8.39	71.32	1.96	1.01	0.10	0.13	0.00	0.02
Series B 1											
B1-0.1+0.063	1.95	0.00	9.00	6.22	79.12	5.40	0.90	0.23	0.08	0.10	0.26
B1-0.063+0.05	1.91	0.00	9.50	4.64	76.24	9.08	0.81	0.20	0.07	0.19	0.29
B1-0.05	2.07	0.00	9.41	5.04	78.38	6.24	1.10	0.20	0.05	0.16	0.24
Series K2											
K2 -0.16+0.1	2.51	0.00	4.94	0.06	88.28	4.03	1.16	0.10	0.40	1.28	0.03
K2- 0.1+0.063	2.37	0.00	6.36	0.62	85.06	4.98	2.02	0.81	0.10	0.57	0.03
K2-0.063+0.05	2.43	0.00	7.86	0.05	83.17	5.65	1.90	0.15	0.39	1.39	0.05
K2 -0.05	1.99	0.50	5.02	0.91	84.46	6.70	3.63	0.13	0.07	0.00	0.36
Series S1											
S1-0.4+0.2	1.87	0.00	4.00	1.90	85.20	8.69	1.00	0.25	0.07	0.18	0.25
S1-0.2+0.16	1.93	0.00	2.48	1.20	88.42	7.43	0.81	0.20	0.05	0.19	0.21
S1-0.16+0.1	2.33	0.00	1.26	0.83	92.52	4.90	1.30	0.11	0.04	0.17	0.27
S1-0.1+0.063	2.44	0.00	1.30	0.92	90.47	6.60	0.90	0.20	0.06	0.18	0.28
S1-0.063+0.05	2.57	0.00	1.35	1.02	89.25	6.70	0.81	0.24	0.10	0.12	0.28
S1-0.05	2.54	0.00	0.64	0.92	89.12	8.81	0.60	0.10	0.05	0.16	0.25

dependences of these characteristics on the iron content in the obtained narrow fractions of ferrospheres are shown in Fig. 3. It can be seen from this figure that, with an increase in the iron content, both the pycnometric and bulk densities increase monotonically and reach maximum values for the S1 series (Berezovsky coal). It should be noted that there is a satisfactory agreement of the presented physical characteristics with ferrospheres of the K series (Irsha-Borodinsky coal), which were investigated in our earlier work²⁴. Moreover, it is important to note that the character of variations in the thermodynamically calculated densities of the melt, from which the ferrospheres are formed, coincides with that of the experimental true densities of the glass-crystalline material of ferrospheres over a wide range of their composition (Fig. 3a). The specific surface area of the ferrospheres decreases rather drastically with an increase in the iron concentration and reaches minimum values 0.17–0.30 m²/g for fractions of the S1 series (Fig. 3b).

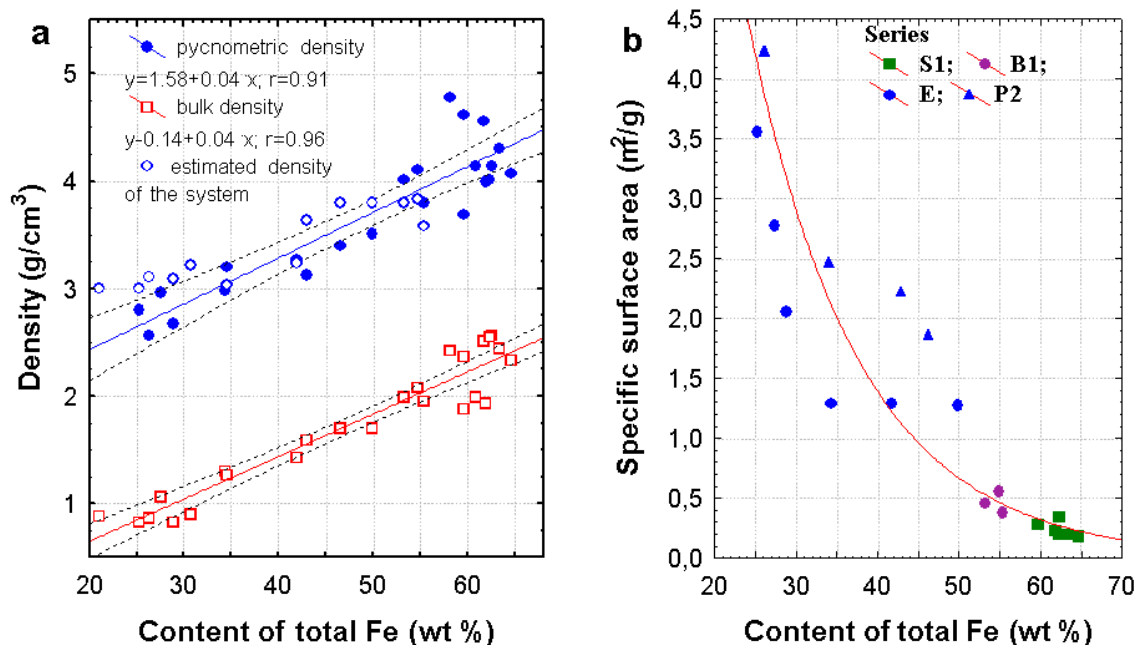


Fig. 3. Dependences of (a) (●) pycnometric and (□) bulk densities and (b) specific surface area of the narrow fractions of ferrospheres on the total iron content.

3.1. Chemical Composition of Ferrospheres

The investigation of the chemical composition of the products obtained has demonstrated that the content of the major components varies over a wide range Fe₂O₃ (30–90 wt %), SiO₂ (0.6–41.6 wt %), Al₂O₃ (0.05–16.32 wt %), and CaO (1.96–9.08 wt %) (Table 1), which overlaps the range of compositions of all the previously studied fractions of the Fs of magnetic concentrations^{3, 5–11} and individual globules⁸.

For analyzing the influence of the chemical composition on the phase composition, morphology of globules, and their properties, the composition dependence of the

content $\text{Al}_2\text{O}_3 = f(\text{Fe}_2\text{O}_3)$ (Fig. 4) is of the most interest. On the one hand, these oxides participate in the formation of magnesium aluminum ferrosphinel of variable composition, which determines the magnetic properties of narrow fractions. On the other hand, both of these components, together with SiO_2 , are involved in the composition of the glass phase and can be differently affect the morphology of the globules. Therefore, the dependence $\text{SiO}_2 = f(\text{Fe}_2\text{O}_3)$ is also of interest.

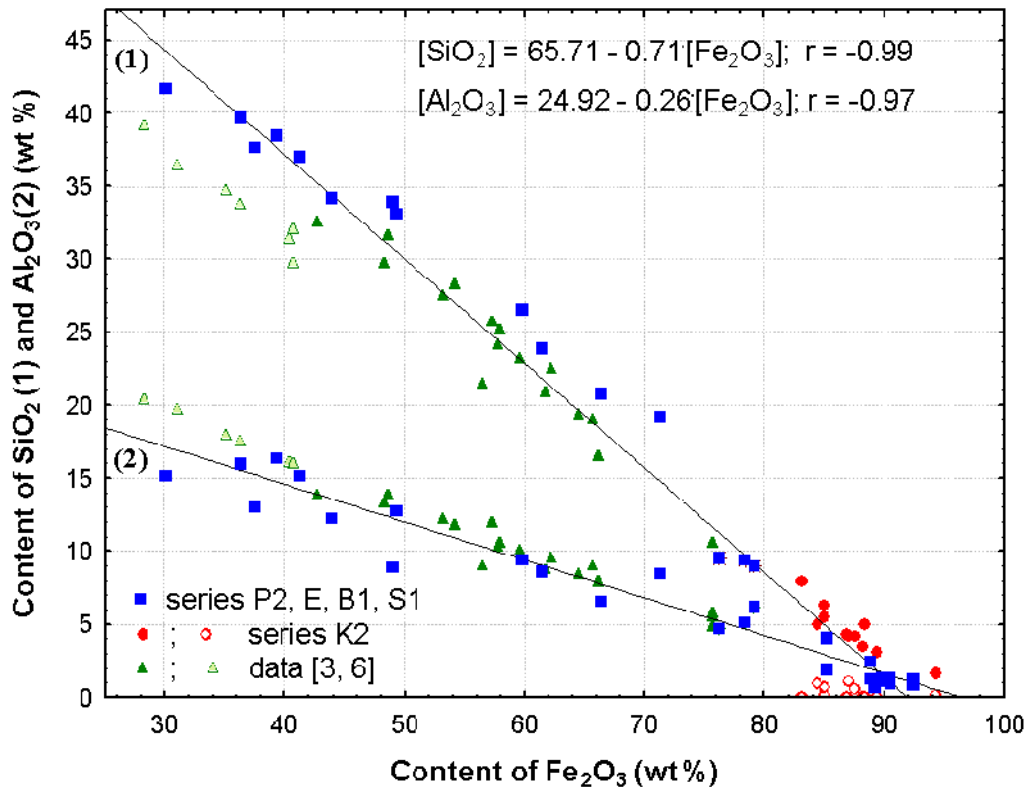


Fig. 4. Dependences of the silicon and aluminum oxide contents in narrow fractions of ferrospheres on the total iron oxide content.

The presented general dependence of the major component composition allows us to separate two types of ferrospheres different in their behavior. The first type includes ferrospheres of the series P2, E, B1, and S1 and is characterized by linear dependences of the contents of SiO_2 and Al_2O_3 on the Fe_2O_3 concentration over a wide range (30.0–92.5 wt %). The second type includes high-iron ferrospheres with an anomalously low (< 1 wt %) content of Al_2O_3 , which were separated from the high-calcium ashes produced from the combustion of brown coals from the Kansk-Achinsk Basin (series K2 and S1).

The major component composition of ferrospheres of the series P2, E, B1, and S1 is described by two linear regression equations $[\text{SiO}_2] = 66.34 - 0.71 \cdot [\text{Fe}_2\text{O}_3]$ and $[\text{Al}_2\text{O}_3] = 24.05 - 0.25 \cdot [\text{Fe}_2\text{O}_3]$ with correlation coefficients of -0.99 and -0.97 , respectively. At the

same time, the data available in the literature ³, which are plotted in the same coordinates and characterize the purified magnetic concentrates obtained from 14 heat and electric power plants in Russia, Ukraine, and Kazakhstan are described by two regression equations $[\text{SiO}_2] = 67.98 - 0.77 \cdot [\text{Fe}_2\text{O}_3]$ and $[\text{Al}_2\text{O}_3] = 26.76 - 0.28 \cdot [\text{Fe}_2\text{O}_3]$ with correlation coefficients of -0.96 and -0.96 respectively. The close purities of the products ³ and the studied narrow fractions of ferrospheres, the same chemical method of analysis of the products, and the close values of the coefficients in the regression equation allow us to combine these two sets of data. The regression equation for the combined set of data corresponds to $[\text{SiO}_2] = 65.71 - 0.71 \cdot [\text{Fe}_2\text{O}_3]$ and $[\text{Al}_2\text{O}_3] = 24.92 - 0.26 \cdot [\text{Fe}_2\text{O}_3]$ with correlation coefficients of -0.99 and -0.97 , respectively.

For compositions of magnetic concentrates obtained from four large electric power plants in Spain ⁶, although the linear dependence is retained, the coefficients of the regression equations $[\text{SiO}_2] = 56.34 - 0.62 \cdot [\text{Fe}_2\text{O}_3]$ and $[\text{Al}_2\text{O}_3] = 30.83 - 0.36 \cdot [\text{Fe}_2\text{O}_3]$ ($r = -0.97$ and -0.99) differ rather significantly from the coefficients of the combined set of data for purified concentrates and narrow fractions of ferrospheres separated from fly ashes of different classes. This difference is most likely associated with the presence of foreign impurities identified by the SEM method ⁶.

The general linear character of the relationship of the major component compositions of the ferrospheres obtained from the combustion of different types of coals allows us to conclude that, during the combustion of coals in heat and electric power plants, all iron forms of the mineral component of the coal participate in the formation of melt droplets whose composition after the partial oxidation and crystallization corresponds to the composition of the concentrates or narrow fractions of the ferrospheres. The composition and content of the iron-containing mineral forms of coals affect only the yield of magnetic concentrates and narrow fractions of particular sizes.

Under the conditions of high temperatures ($> 1200^\circ\text{C}$) and the reducing medium of the core of the flame, iron exists in the form of Fe^{2+} and can form eutectics over a wide range of compositions of ternary and quaternary systems ^{8, 39}. During cooling and with an increase in the oxidation potential, there occurs a partial oxidation of Fe^{2+} into Fe^{3+} , and iron precipitates from silicate melts, predominantly, in the form of the ferrosphinel of the base composition of magnetite Fe_3O_4 or its mixture with $\alpha\text{-Fe}_2\text{O}_3$ ⁸.

For the Fe_2O_3 content ranging from 36 to 70%, the main components in the composition of the melt are FeO , SiO_2 , and Al_2O_3 (in order of decreasing content); among these systems are microspheres of the series E and P2. When the Fe_2O_3 content is approximately equal to 80% (series B1), the content of SiO_2 and Al_2O_3 becomes comparable to the CaO content and, consequently, the behavior of the melt is determined by the properties of the $\text{FeO}\text{-SiO}_2\text{-Al}_2\text{O}_3\text{-CaO}$ system. In the case of high-calcium ashes for the Fe_2O_3 content ranging from 76 to 92 wt % and a low Al_2O_3 content (< 1 wt %) (series K2 and S1), the behavior of the melt is determined by the properties of the $\text{FeO}\text{-CaO}$ system.

3.2. Phase Composition of Ferrospheres

The formation of ferrospheres in such different systems of complex composition should lead to significant differences in their phase compositions. According to the paper ⁶, the main phases (> 10%) in the magnetic fraction are the iron-enriched aluminosilicate glass, magnetite, quartz, and hematite, as well as mullite, plagioclase, ferrite spinel, and char particles at a level of 1–10%. The magnetite content is usually higher than the hematite content; however, the ratio of these phases in ferrospheres from different fly ashes somewhat changes ^{6, 9, 10}. In the magnetic fractions produced from ashes of bituminous coals, the dominant phases are the glass phase (50.0–71.5%) and spinel (24.0–47.8%) with impurities of quartz and coke ⁷ or the amorphous phase (54.4%) and mullite (25.1%) with impurities of quartz, potassium feldspar, calcite, hematite, and magnetite with magnesium ferrite and hercynite ¹¹.

The main phase of the narrow fractions of Fs (Table 2) is the magnetite-based spinel phase with the content ranging from 25 до 82 wt %; in this case, the content of the spinel phase increases linearly with an increase in the iron content in Fs (Fig. 5a). All samples also contain hematite, and its content is substantially lower in microspheres of the series E, P2, and B1 as compared to those of the series K2 and, especially, S1.

The phase composition of the Fs with a high content of silicon and aluminum (series E and P2) includes mullite $3\text{Al}_2\text{O}_3 \cdot 2\text{SiO}_2$, quartz $\alpha\text{-SiO}_2$, and the glass phase with a high concentration (up to 56.5 wt %) (Table 2). A decrease in the content of silicon and aluminum leads to the disappearance of the mullite phase in the composition of microspheres of the series B1, S1, and K2; in this case, the content of the quartz and amorphous phases decreases significantly.

Apart from the differences in the phase compositions of Fs of different series, there are also differences in the microstructures of ferrospheral and hematite. The X-ray diffraction studies of the narrow fractions of Fs (Table 2, Fig. 5b) have demonstrated that, for Fs of the series E, P2, and B1, which are formed from the $\text{FeO-SiO}_2\text{-Al}_2\text{O}_3$ melt, the preferential crystallization is observed for the ferrospheral phase in which the unit cell parameter monotonically increases in the range from 8.344 to 8.3897 Å with an increase in the iron content and almost reaches the value 8,396 Å, which is characteristic of magnetite. In this case, the observed increase in the unit cell parameter is explained by the gradual isomorphous substitution of Al and Mg ions in the spinel structure for the Fe ions.

For ferrospheres of the series K2 and S1, which are formed from the calciowustite melt, calcium during partial oxidation can isomorphously substitute for iron in the magnetite structure, but only in limited amounts. According to estimates ⁴⁰, the content of CaFe_2O_4 , which forms a homogeneous solid solution with FeFe_2O_4 , reaches 14 mol %. The saturation of magnetite by calcium ferrite is favored by an increase in the oxygen potential and an increase in the basicity of the medium. As the temperature decreases, the $(\text{Ca,Fe})\text{Fe}_2\text{O}_4$ solid solutions decompose. The calcium ferrites precipitate in the form of individual phases in the magnetite matrix.

Table 2. Phase composition and unit cell parameters of the phases of ferrospheres

Series, fraction	Phase composition, wt %								Unit cell parameter, Å		
	Ferrosipinel	Hematite	Quartz	Calcite	Mullite	ϵ -Fe ₂ O ₃	FeO	Amorphous phase	Ferrosipinel	Hematite	
									a	a	b
Series P2											
P2-0.16-0.1	19.9	1.7	8.7	2.8	4.3	0.3	-	62.4	8.360(4)	5.032(1)	13.728(3)
P2-0.1+0.063	35.5	1.9	5.7	0.6	1.8	0.4	-	54.1	8.365(3)	5.029(1)	13.737(4)
P2-0.063+0.05	41.1	2.7	4.9	0.4	1.6	0.5	-	48.9	8.371(2)	5.034(1)	13.728(4)
P2-0.05	52.5	7.3	2.4	0.1	0.7	2.0	-	35.1	8.368(1)	5.0316(4)	13.732(2)
Series E											
E-0.4+0.2	26.0	1.8	5.7	0.4	12.1	0.3	-	53.8	8.348(2)	5.026(2)	13.714(6)
E-0.2+0.16	30.0	1.1	5.4	0.2	12.4	0.4	-	50.6	8.344(2)	5.032(3)	13.710(7)
E-0.16+0.1	37.7	2.4	4.7	0.5	7.5	0.5	-	46.8	8.359(1)	5.029(1)	13.727(4)
E-0.1+0.063	43.7	2.0	4.3	0.1	4.9	0.3	-	44.8	8.363(1)	5.032(2)	13.719(4)
E-0.063+0.05	48.8	2.9	3.1	0.1	3.5	0.4	-	41.2	8.366(1)	5.032(1)	13.727(4)
E-0.05	45.6	4.3	2.6	0.0	2.9	2.8	-	41.8	8.360(1)	5.0302(6)	13.729(3)
Series B1											
B1-0,1+0,063	69.4	2.6	1.2	-	-	-	0.8	26.0	8.3897(2)	5.0327(5)	13.737(1)
B1-0,063+0,05	67.0	3.8	1.3	-	-	-	0.6	27.2	8.3876(2)	5.0322(4)	13.737(1)
B1-0,05	65.4	5.9	1.7	-	-	-	0.3	26.8	8.3851(2)	5.0322(5)	13.730(2)
Series K2											
K2-0.16+0.1	70.2	12.4	2.3	-	-	-	-	15.2	8.4073(5)	5.0346(2)	13.7448(7)
K2-0.1+0.063	67.1	13.3	2.5	-	-	-	-	17.1	8.4068(5)	5.0350(2)	13.7463(7)
K2-0.063+0.05	66.8	13.4	2.6	-	-	-	-	17.2	8.4061(5)	5.0348(2)	13.7445(7)
K2-0.05	69.4	5.3	1.8	-	-	-	-	23.5	8.4047(5)	5.0354(5)	13.740(1)
Series S1											
S1-0,4+0,2	64.7	10.1	1.3	-	-	-	-	23.8	8.3959(2)	5.0340(5)	13.748(1)
S1-0,2+0,16	63.6	18.7	1.3	-	-	-	-	16.4	8.3957(2)	5.0328(3)	13.7445(5)
S1-0,16+0,1	65.8	24.6	0.7	-	-	-	-	9.0	8.3994(2)	5.0343(3)	13.7461(5)
S1-0,1+0,063	54.8	22.6	0.5	-	-	-	-	22.1	8.3991(2)	5.0347(3)	13.7455(5)
S1-0,063+0,05	44.6	35.6	0.5	-	-	-	-	19.3	8.3982(2)	5.0346(3)	13.7466(5)
S1-0,05	38.2	37.5	0.4	-	-	-	-	23.8	8.3951(3)	5.0347(1)	13.7469(2)

According to the paper ⁴¹, during the crystallization of the Fe₂O₃-Fe₃O₄-CaO melt, the formed magnetite is noticeably doped and has the Fe_{2.9}Ca_{0.1}O₄ composition with the lattice parameter $a_0 = 8.430$ Å. Moreover, the substantial concentration of calcium is observed at crystal grain boundaries. Upon the formation of high-calcium ferrospheres in the presence of sufficient amounts of SiO₂, the calcium iron silicate glass phase

(series B1 and K2) is formed at boundaries of the crystalline phases for binding free calcium. In the absence of SiO₂ in the system, CaO is concentrated at boundaries of the crystalline phases (series S1).

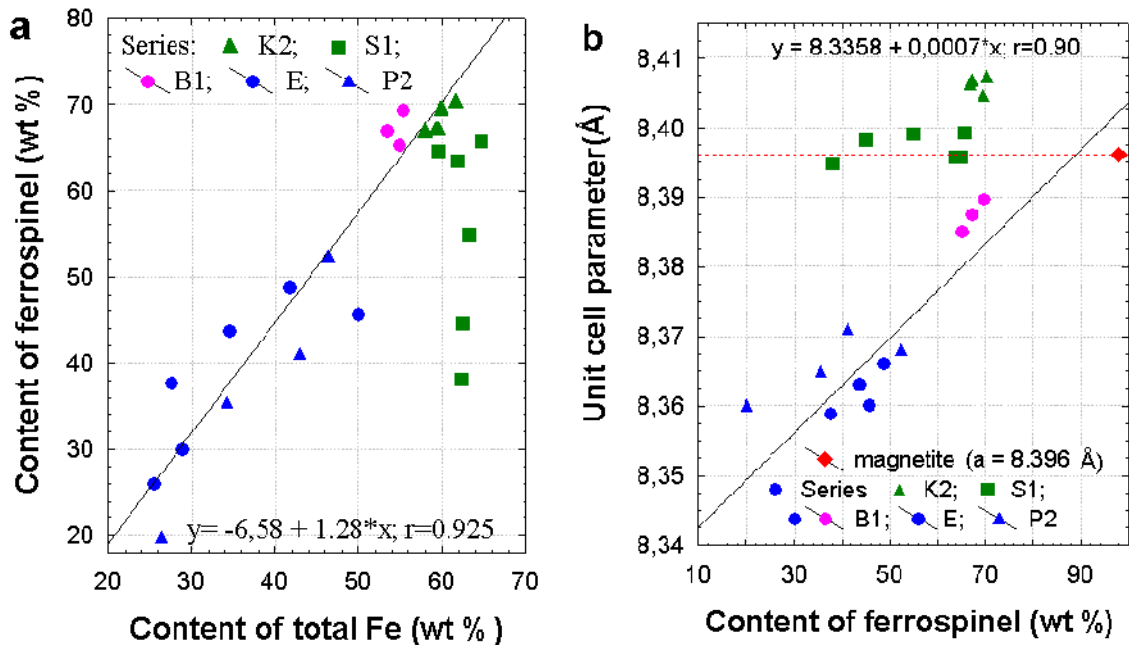


Fig. 5. Dependences of (a) the content of the ferrosphinel phase on the total iron content and (b) the unit cell parameter of the ferrosphinel on the ferrosphinel content in narrow fractions of ferrospheres.

A rapid cooling of microdroplets of the melt can stabilize the (Ca,Fe)Fe₂O₄ spinels in the composition of ferrospheres of the series S1 and K2. This apparently can explain both the high values of the unit cell parameter in the ranges 8.3951–8.3994 Å for the S1 series and 8.4047–8.4073 Å for the K2 series, which exceed the corresponding parameter of stoichiometric magnetite, and the formation of defect structures revealed by Mössbauer spectroscopy.

Thus, two different classes of microspheres can be separated over a wide range of variations in the composition of the prepared ferrospheres. One of them (series E, P2, and B1) are formed from the FeO–SiO₂–Al₂O₃ melt and include aluminum magnesium ferrosphinel of variable composition. The other microspheres (series K2 and S1) are formed in the CaO–FeO system and include (Ca,Fe)Fe₂O₄ and hematite with the CaO oxide concentrated on their surface. The differences in the compositions and conditions of the formation of ferrospheres should affect not only the phase composition but also the morphology of the globules and the catalytic properties of ferrospheres.

3.3. Relationship between the Composition and Morphology of Ferrospheres

The formation of microspherical globules proceeds at the high-temperature stage due to the complete or partial melting of the ferrospheres material, and the structural features

depend primarily on the processes of phase formation inside the globules. It should be noted that, owing to the temperature gradient and the specific features of the phenomena occurring at the phase boundaries, the surface structures could differ from the bulk structures.

As the Fe_2O_3 content increases from 36 to 92 wt %, the main morphological type of globules in the magnetic microspheres change in the following order: porous (foam-like) with different porosities of the bulk – glass-like with a poorly pronounced dendritic structure – dendritic – skeleton-dendritic – monolithic large block-like (Fig. 6).

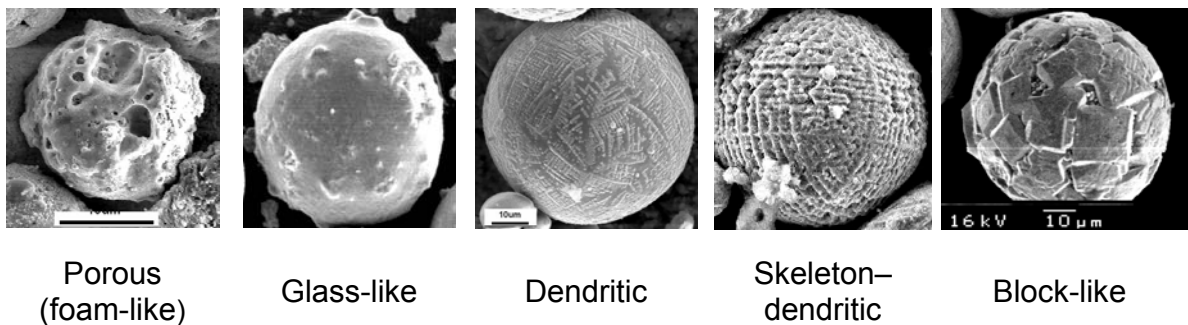


Fig. 6. Main morphological types of ferrospheres.

In addition to the massive globules, all fractions of microspheres include plerospheres that have different thicknesses and different textures of the shells (Fig. 7). The formation of such globules proceeds under the conditions of considerable temperature gradient when the outer layer has managed to melt and, inside the globules, small microspheres and particles, or their aggregates, are encapsulated⁴². In the study of single plerospheres⁹, it was shown that small magnetic microspheres can be encapsulated together with weakly magnetic and nonmagnetic particles in the shell of the aluminosilicate composition (< 5.46% Fe_2O_3).

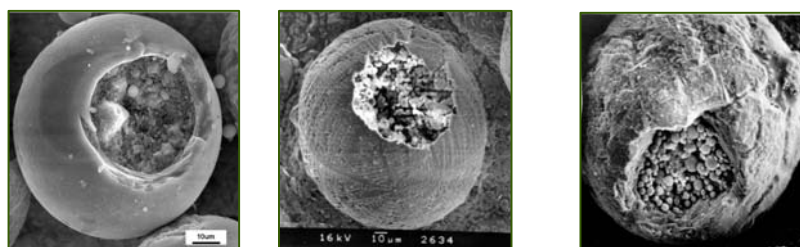


Fig. 7. Main morphological types of plerospheres.

3.4. Catalytic Properties of Narrow Fractions of Ferrospheres

For all the studied samples, the noticeable conversion of the components of the reaction mixture, namely, methane and oxygen, was observed at temperatures above 600°C. The catalytic activity of the studied samples in the reaction of oxidative conversion of methane was changed over wide ranges. The quantitative characteristic of the catalytic activity was taken to be the conversion (x_{ox}) of oxygen as a deficient component in the reaction mixture. Incidentally, the dependence of the methane conversion (x_m) on the iron content was qualitatively similar to the corresponding curves for oxygen, but the changes were less pronounced: with variations in x_{ox} in the range 0–100%, the corresponding variations in x_m did not exceed 8%.

The dependence of the catalytic activity of ferrospheres on the total iron content (C_{Fe}) in the samples at temperatures of 650 and 700°C is shown in Fig. 8. Despite the considerable spread of the experimental data about the trend line, it is obvious that, with an increase in the total iron content C_{Fe} , the activity changes regularly and these variations have a complex nonmonotonic character. For the values of C_{Fe} in the range 45–50 wt %, we observed a maximum of the total activity, which is characteristic of all temperatures and is most clearly pronounced at 700°C (Fig. 9).

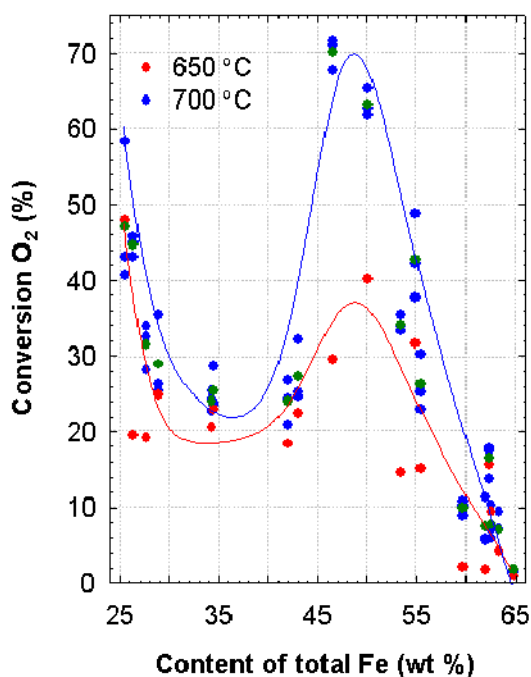


Fig. 8. Dependence of the catalytic activity of ferrospheres (conversion of O_2) at temperatures of 650 (●) и 700 °C (●) on the total iron content in ferrospheres.

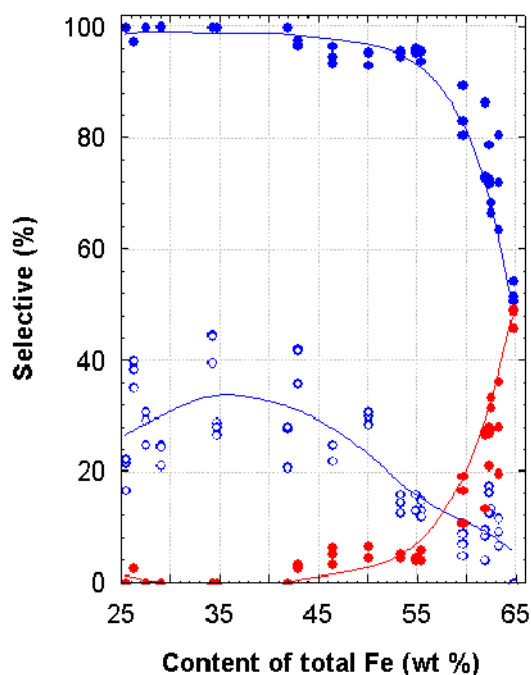


Fig. 9. Selectivity of the formation of products of the oxidative conversion of methane as a function of the total iron content in ferrospheres at a temperature of 700°C: (●) sum of C_2 hydrocarbons, (○) CO, and (●) COx.

Apart from the activity, the selectivity of the methane conversion also substantially depends on the iron content (Fig. 8). The main products of the CH₄ conversion for the samples with $C_{Fe} < 56$ wt % are CO and CO₂, and their ratio varies with an increase in C_{Fe} . For the samples with iron concentrations above 56 wt %, we observed the formation of products of the oxidative dimerization, namely, ethane and ethylene, as well as C₃ hydrocarbons. In this region of compositions of Fs the selectivity of the formation of products of the oxidative dimerization increases with increasing temperature, and at a constant temperature, the selectivity with respect to C₂ hydrocarbons increases proportionally with C_{Fe} and reaches 60% at a temperature of 750°C for the samples with a high iron content.

Therefore, reasoning from the data presented in Figs. 8 and 9, all ferrospheres, according to their behavior in the reaction of oxidative conversion of methane, can be conventionally divided into three groups:

- Group I. This group includes samples of the series E and P2, for which $C_{Fe} < 45$ wt %. The activity of these ferrospheres is not very high, and the dominant contribution comes from the reaction of deep oxidation of methane.
- Group II. Samples of the second group are Fs of the B1 series –0.05 mm and samples of the series E and P2 ($C_{Fe} = 45\text{--}50$ wt %). These Fs are active but low-selectively catalysts of the oxidative dimerization, on which there occur predominantly the processes of deep oxidation of methane to CO₂, and the maximum activity is observed for Fs with the Fe₂O₃ content approximately equal to 50 wt %.
- Group III. Samples of the third group are Fs of the S1 series with the iron content above 56 wt %. These Fs are characterized by an increased selectivity of the formation of C₂ products (30–60%), which increases with an increase in the total iron content.

As was already noted above, Fs of the series E, P2, and B1 are formed from the FeO–SiO₂–Al₂O₃ melt and include the magnesium aluminum ferrosphal with the content monotonically increasing with an increase in the iron content in Fs. Spinel of this type are effective catalysts of deep oxidation of methane⁴³. In the series of studied ferrospheres, an increase in C_{Fe} led to a drastic decrease in the specific surface area (Fig. 1b), which is determined by the porosity of the glass phase. Therefore, the low activity of the first group of ferrospheres ($C_{Fe} < 45$ wt %) is explained by a combination of two factors: (i) the relatively low content of the active spinel phase and (ii) the high content of the glass phase, which blocks the surface of the catalytically active ferrite spinel.

Owing to the decrease in the size of globules (fractions –0.05 mm of the series E and P2) and the substantially lower content of the glass phase in Fs of the B1 series, the catalytically active phase of the spinel becomes accessible. Therefore, ferrospheres of the second group exhibit the highest activity in the reaction of deep oxidation of methane.

The most surprising is the fact of the significant decrease in the activity in the reaction of deep oxidation and an increase in the selectivity with respect to C_2 products of the reaction of oxidative dimerization for Fs of the S1 series at high iron concentrations, i.e., under the conditions where the system is dominated by the hematite and ferrosphenel phases, which are known as catalysts of deep oxidation^{25, 44}.

In the case of Fs of the S1 series, the lattice parameter of the ferrosphenel exceeds the lattice parameter a_0 for magnetite and reaches 8.3994 Å, which indicates the possibility of forming Ca-doped solid solutions based on Fe_3O_4 . The bulky Ca^{+2} ion with a higher probability should be incorporated into octahedral positions of the structure, which are able to accommodate cations of a larger radius. Detailed investigations of a series of substituted spinels⁴⁴ have shown that their activity in the reaction of deep oxidation is primarily determined by the nature of Me^{+3} cations located in octahedral positions. It was also noted that the modification of the structure with respect to the B position changes the redox properties of the surface, possibly, due to the variations in the mobility of the lattice oxygen⁴⁵. Therefore, it can be expected that doping of magnetite by calcium ions should lead to a significant change in the level of activity of the ferrite spinel.

Unfortunately, catalysts with a spinel structure have very rarely used in the investigation of the process of oxidative dimerization of methane. To the best of our knowledge, there is only one work in which catalysts with a spinel structure were used in the explicit form during the oxidative dimerization of methane⁴⁶. It was shown, in particular, that $ZnFe_2O_4$ exhibits an average level of activity in the oxidative dimerization of methane at a temperature of 800°C, and the conversion of methane x_{CH_4} in the reaction mixture of 41.6% CH_4 and 8.4% O_2 reaches 20% when the yield of hydrocarbons y_{C_2} is approximately equal to 13% and the selectivity of the formation of C_2 hydrocarbons amounts to ~ 65% of the corresponding selectivity of the ferrospheres.

Moreover, if we assume by analogy with^{40, 41} that, during the crystallization of Fs (series S1), calcium is also displaced toward the surface of the $(Ca,Fe)Fe_2O_3$ and Fe_2O_3 crystallites, the low activity in the deep oxidation and the high selectivity of the formation of C_2 hydrocarbons can be explained by the catalytic properties of the surface enriched in CaO.

It is known that promoted CaO is a rather effective system in the process of oxidative dimerization of methane at a temperature of 700°C^{47, 48}. The use of alkali promoters increases the activity of CaO in the oxidative conversion of methane with an increase in the concentration of Fe^{3+} impurity ions in the CaO matrix. An increase in the fraction of $M^+CO_3^{2+}$ centers in promoted CaO leads to an increase in the selectivity of the formation of C_2 hydrocarbons (to 60%) in the CH_4-O_2 reaction medium.

Thus, the activity of Fs of the S1 series in the formation of CO_2 can be explained by the blocking of centers providing the deep oxidation of CH_4 due to the enrichment of the CaO surface and by the formation of new centers

responsible for the high selectivity of the formation of C₂ hydrocarbons from methane.

CONCLUSIONS

(1) The systematic investigation the relationship between the composition, morphology, structural characteristics of iron-containing phases, and catalytic properties of narrow fractions of Fs separated from four known types of fly ashes has been performed.

(2) It has been established that the major component compositions of all the studied narrow fractions of Fs and magnetic concentrates obtained from 14 heat and electric power plants in Russia, Ukraine, and Kazakhstan are described by two general linear regression equations $[\text{SiO}_2] = 65.71 - 0.71 \cdot [\text{Fe}_2\text{O}_3]$ and $[\text{Al}_2\text{O}_3] = 24.92 - 0.26 \cdot [\text{Fe}_2\text{O}_3]$ with correlation coefficients of -0.99 and -0.97 , respectively. This means that all iron-containing mineral components of coals are mobilized upon the formation of ferrospheres. The composition and content of the iron-containing mineral forms of the original coal affect the yield of the magnetic concentrates and narrow fractions of particular size and composition.

(3) In the general dependence of the Fs composition, there are two regions different in the properties of the melt from which the Fs are formed. In a wide range of variations in the iron concentration $C_{\text{Fe}} = 25\text{--}55$ wt %, the behavior of the melt is determined by the properties of the FeO–SiO₂–Al₂O₃–CaO system. For higher iron concentrations $C_{\text{Fe}} > 55$ wt % and low contents of Al₂O₃ and SiO₂ (< 1 wt %), the behavior of the melt is determined by the properties of the FeO–CaO system.

(4) The FeO–SiO₂–Al₂O₃–CaO system is characterized by the formation of aluminum magnesium ferrosphinel. The content of the ferrosphinel increases with increasing iron concentration, and the unit cell parameter of the ferrosphinel changes in the range 8.344–8.3897 Å. The activity of the Fs in the reaction of deep oxidation of methane is determined by the ferrosphinel concentration and the content of the glass phase in narrow fractions of Fs. The high content of the amorphous phase leads to a blocking of the catalytically active ferrosphinel and to a decrease in the activity of the Fs.

(5) The FeO–CaO system is characterized by the formation of CaO-promoted ferrosphinel, which has the unit cell parameter exceeding the corresponding parameter of stoichiometric magnetite, and by the formation of defect $\alpha\text{-Fe}_2\text{O}_3$ with the surface enriched in CaO. The drastic change observed in the catalytic properties of Fs in this system is explained by the enrichment of the surface of iron-containing CaO phases and by the formation of defect centers responsible for the high selectivity in the reaction of oxidative dimerization of methane.

ACKNOWLEDGMENTS

We would like to thank E.V. Kondratenko (Leibniz Institute of Catalysis at the University of Rostock, Germany) for his assistance in performing the catalytic studies.

This study was supported by the Siberian Branch of the Russian Academy of Sciences within the framework of the Interdisciplinary Integration Project No. 77.

REFERENCE

- [1] Hansen, L.D., Silberman, D. and Fisher, G.L. *Environ. Sci. Technol.*, 1981, 15, pp.1057-1062.
- [2] Raask, E. *Mineral impurities in coal combustion: Behavior, problems and remedial measures*. Hemisphere, Washington, DC, 1985, p. 484.
- [3] Kizil'shtein, L.Ya., Dubov, I.V., Shpitsgluz, A.L., Parada, S.G. *Components of ashes and slags of heat power plants*, Energoatomizdat, Moscow, 1995, p. 176 [in Russian].
- [4] Vassilev, S.V., Vassileva, C.G. *Fuel Process Technol.*, 1996, 47, pp. 261-280.
- [5] Vassilev, S.V. *Fuel*, 1992, 71, pp.625-633.
- [6] Vassilev, S., Menendez, R., Borrego, A., Diaz-Somoano, M., Martines-Tarazona, M. *Fuel*, 2004, 83, pp. 1563-1583.
- [7] Hower, J., Rathbone, R., Robertson, J., Peterson, G., Trimble, A. *Fuel*, 1999, 78, pp. 197-203.
- [8] Sokol, E.V., Kalugin, V.M., Nigmatulina, E.N., Volkova, N.I., Frenkel, A.E., Maksimova, N.V. *Fuel*, 2002, 81, pp. 867-876.
- [9] Kukier, U., Ishak, C.F., Sumner, M.E., Miller, W.P.P. *Environmental Pollution*, 2003, 123, pp. 255-266.
- [10] Bibby, D., *Fuel*, 1977, 56, pp. 427-431.
- [11] Dai S., Zhao L., Peng S., Chou Ch-L., Wang X., Zhan Yg., Li D., Sun Y. *J. of Coal Geology*, 2009.doi:10.1016 j.coal.2009.03.005
- [12] Hulett, L., Weinberger, A., Northcutt, K., Ferguson, M., *Science*,1980, 210, pp.1356-1358.
- [13] Pat. 4 191 336 US, 1980.
- [14] Pat. 4 432 868 US, 1984.
- [15] Pat. 3 769 054 US, 1973.
- [16] Pat. 4 386 057 US, 1980.

- [17] Pavlenko, V.I., Sokolova, V.S., Strokova, V.V., Basmanov, G.V. The cement-magnetite composites for conservation of radioactive wastes from nuclear power stations. Publ. BelGTASM, Belgorod, 2002, p.154 [in Russian].
- [18] Pat. 4 698 289 US, 1987.
- [19] Frank, L.A., Borisova, V.V., Vereshchagina, T.A., Fomenko, E.V., Anshits, A.G., Gitelson, I.I. Appl. Biochem. Microbiol., 2009, 45(2), pp. 215-220.
- [20] Sharonova, O.M., Akimochkina, G.V., Rabchevskii, E.V., Kryuchek, D.M., Anshits, A.G. Proceedings VII Intern. Conf. "Safety of Nuclear Technologies: Radioactive Waste Management", Pro Atom, Saint-Petersburg, 2004, pp. 470-474.
- [21] Pat. 2 375 410 RU, 2009.
- [22] Pat. 2 375 412 RU, 2009.
- [23] Anshits, A.G., Kondratenko, E.V., Fomenko, E.V., Kovalev, A.M., Anshits, N.N., Baykov, O.A., Sokol, E.V., Salanov, A.N. Catal.Today, 2001, 64, pp. 59-67.
- [24] Fomenko, E.V., Kondratenko, E.V., Salanov, A.N., Bajukov, O.A., Talyshev, A.A., Maksimov, N.G., Nizov, V.A., Anshits, A.G. Catal. Today, 1998, 42, pp. 267-272
- [25] Fomenko, E.V., Kondratenko, E.V., Sharonova, O.M., Plekhanov, V.P., Koshcheev, S.V., Boronin, A.I., Salanov, A.N., Bajukov, O.A., Anshits, A.G. Catal. Today, 1998, 42, pp. 273-277.
- [26] Vdovchenko, V.S., Martynova, M.I., Novitskii, N.V., Jushina G.D. Handbook. Energy fuel of the USSR. Energoatomizdat, Moscow, 1991, p. 184 [in Russian].
- [27] Eremin, I.V., Bronevets, T.M. Handbook. Rank composition of coal and its rational use. Nedra, Moscow, 1994, p. 254 [in Russian].
- [28] State standard GOST 25543-88. Brown coals, hard coals and anthracites. Classification according to genetic and technological parameters. 1988. [in Russian].
- [29] ASTM D388-98a. Standard Classification of Coals by Rank, 2005.
- [30] Vassilev, S.V., Vassileva, C.G. Fuel, 2007, 86, pp.1490-1512.
- [31] Pat. 2 407 595 RU, 2010.
- [32] Pat. 2 129 470 RU, 1999.
- [33] State standard GOST 23148-98. Powders for powder metallurgy. Sampling [in Russian].

- [34] State standard GOST 5382-91. Cements and materials for cement production. Chemical analysis methods [in Russian].
- [35] State standard GOST 16190-70* Sorbents. Method for determination of bulk density [in Russian].
- [36] State standard GOST 18318-94. Metallic powders. Determination of particles size by dry sieving. 1994. [in Russian].
- [37] Rietveld H.M. J. Appl. Crystallogr., 1969, 2, pp. 65-71.
- [38] Solovyov L.A. J. Appl. Crystallogr., 2004, 37, pp. 743-749.
- [39] Bruant, G., Bailer, C., Wu, H., McLennan, A., Stanmore, B., Wall, T. Iron in coal and slagging. The significance of the high temperature behaviour of siderite grains during combustion, Springer US, DOI 10.1007/B118076. pp.581-591
- [40] Eitel W. Physical chemistry of the silicates. University of Chicago Press, Chicago, 1954; Inostrannaya Literatura, Moscow, 1961, p. 1055.
- [41] Orewczyk, J. J. Thermal Anal. and Calorimetry, 2000, 60, pp. 265-269.
- [42] Fisher, G.L., Chang, D.P.Y., Brumer, M. Science, 1976, 192, pp. 553-555.
- [43] Boreskov, G.K., Popovskii, V.V., Lebedev, N.I., Sazonov, V.A., Andrushkevitch, T.V. Kinet. i Katal., 1970, 11(5), p.1253-1261 [in Russian].
- [44] Boreskov G.K. Catalysis. Theoretical and practical problems. Selected Proceedings, translated under the title Kataliz. Voprosy teorii i praktiki. Izbrannyye trudy, Nauka, Novosibirsk, 1987, p.536 [in Russian].
- [45] Zhou, K., Chen, H., Tian, Q., Hao, Z., Shen, D., Xu, X. J. Mol. Catal. A, 2002, 189, pp. 225.
- [46] Papa, F., Patron, L., Carp, O., Paraschiv, C., Ioan, B. J. Molec. Catal. A, 2009, 299, pp.93-97.
- [47] Kondratenko, E.V., Maksimov, N.G., Anshits, A.G. Kinet. i Katal., 1995, 36 (5), pp. 658-662 [in Russian].
- [48] Voskresenskaya, E.N., Roguleva, V.G., Anshits, A.G. Catal. Rev.-Science and Engineering, 1995, 37 (1), pp. 101-143.